Dyes and Pigments 85 (2010) 143–151

Contents lists available at ScienceDirect

Dyes and Pigments

journal homepage: www.elsevier.com/locate/dyepig

Tunable emission of polymer light emitting diodes bearing green-emitting Ir(III) complexes: The structural role of 9-((6-(4-fluorophenyl)pyridin-3-yl) methyl)-9*H*-carbazole ligands

Min Ju Cho [a], Jung-Il Jin [a], Dong Hoon Choi [a,*], Jung Hee Yoon [a], Chang Seop Hong [a], Young Min Kim [b], Young Wook Park [b], Byeong-Kwon Ju [b]

[a] *Department of Chemistry, Advanced Materials Chemistry Research Center, Korea University, 5 Anam-dong, Sungbuk-gu, Seoul 136-701, Republic of Korea*
[b] *Display and Nanosystem Laboratory, College of Engineering, Korea University, 5 Anam-dong, Sungbuk-gu, Seoul 136-701, Republic of Korea*

ARTICLE INFO

Article history:
Received 14 September 2009
Received in revised form
24 October 2009
Accepted 28 October 2009
Available online 31 October 2009

PACS:
78.60.Fi
78.66-w
78.55

Keywords:
Iridium(III) complex
Ligand
Solubility
Photoluminescence
Triplet energy transfer
Electrophosphorescence

ABSTRACT

9-((6-Phenylpyridin-3-yl)methyl)-9*H*-carbazole and 9-((6-(4-fluorophenyl)pyridin-3-yl)methyl)-9*H*-carbazole were synthesized as ligands by attaching a carbazolyl group to the pyridine in 2-phenylpyridine and 2-(4-fluorophenyl)pyridine, respectively. Four different Ir(III) complexes were prepared using a simple procedure, the solubility of which was significantly greater than that of conventional green-emitting $Ir(ppy)_3$. Among the many devices fabricated, that which contained 10% of $Ir(Cz\text{-}ppy)_1(Cz\text{-}Fppy)_2$ in PVK/PBD (70:30 wt%), exhibited an external quantum efficiency of 6.80%, luminous efficiency of 20.23 cd/A, and maximum brightness of 17520 cd/m^2. In particular, the electronic property of the new 9-((6-(4-fluorophenyl)pyridin-3-yl)methyl)-9*H*-carbazole ligand can manipulate the triplet energy level of the Ir(III) complex to finely tune the emission spectra.

1. Introduction

Of the various types of light-emitting organic materials available, phosphorescent materials have been recognized as superior candidates because both singlet and triplet excitons can generate unique light emissions, with a theoretical internal quantum efficiency of 100% [1–3]. In particular, cyclometalated Ir(III) complexes show high phosphorescent efficiencies and are one of the most promising classes of phosphorescent dyes used in organic light-emitting diodes (OLEDs) [4–11]. Along with advancements in processing solutions for the fabrication of OLEDs, novel, highly soluble materials displaying phosphorescence have been reported recently [12–14]. An extensively used technique for enhancing the solubility of Ir(III) complexes is via the attachment of lengthy alkyl moieties or their introduction into dendrimers [15–18]. A dendritic architecture improves both solubility and the site-isolation effect by employing various peripheral groups around the emission center [19,20].

In addition to the above methods, a very promising Ir(III) complex containing the tetraphenylsilyl group has been reported to exhibit excellent luminous efficiency using a conventional polymer-based [poly(*N*-vinyl carbazole), PVK] OLED. The design and synthesis of a highly phosphorescent tris-cyclometallated homoleptic Ir(III) complex [$Ir(TPSppy)_3$] (TPSppy = 2-(4′-(triphenylsilyl) biphenyl-3-yl)pyridine) with a silane-based dendritic substituent have been demonstrated. It has also been suggested that aryl silane was quite effective at emitting UV light for improving device efficiency compared to a long alkyl substituent [21].

Liu et al. reported PVK based light-emitting diodes fabricated with pinene-substituted Ir(III) phosphorescent dopants; three different Ir(III) complex dyes were demonstrated for which a photoluminescent spectral shift was observed with ligand modification. In addition, the pinene substitution induced steric hindrance to molecular structure of the dopant that aided suppression of

* Corresponding author. Tel.: +82 2 3290 3140; fax: +82 2 924 3141.
E-mail address: dhchoi8803@korea.ac.kr (D.H. Choi).

0143-7208/$ – see front matter © 2009 Elsevier Ltd. All rights reserved.
doi:10.1016/j.dyepig.2009.10.017

triplet–triplet annihilation between Ir(III) dyes and consequently improved device performance [22]. These findings suggested that by substituting an electron withdrawing fluorine atom within the ligand, the HOMO energy levels could be tuned, thereby increasing the bandgap energy.

The objective of this work was to explore a method for tuning emission color by combining novel ligand design and good solubility and miscibility of the host polymer. This paper deals with three different highly soluble Ir(III) complexes bearing the 9-((6-phenylpyridin-3-yl)methyl)-9*H*-carbazole and 9-((6-(4-fluorophenyl)pyridin-3-yl)methyl)-*9H*-carbazole ligands. Green electrophosphorescence polymer light-emitting diodes (PLEDs) were fabricated by doping $Ir(Cz\text{-}ppy)_2(Cz\text{-}Fppy)_1$, $Ir(Cz\text{-}ppy)_1(Cz\text{-}Fppy)_2$, or $Ir(Cz\text{-}Fppy)_3$ into PVK blended with 5-4-*tert*-butylphenyl-1,3,4-oxadiazole (PBD), an electron transport molecule. For reference, the $Ir(Cz\text{-}ppy)_3$ was previously reported as being employed to compare the performances of photoluminescence (PL) spectrum and electrophosphorescent devices fabricated under identical conditions [23]. Two different ligands were systematically tethered to form a complex for investigating the effect of an electron withdrawing substituent in the ligand on the photophysical and electrophosphorescent properties.

2. Experimental

2.1. Materials

All commercially available starting materials and solvents were purchased from Aldrich, TCI, and ACROS Co. and used without further purification unless otherwise stated. HPLC grade dimethylformamide (DMF) and methylene chloride (MC) were purchased from Samchun chemical and distilled from CaH_2 immediately before use. All reactions were performed under an argon atmosphere unless otherwise stated. 9-(6-Chloro-pyridin-3-ylmethyl)-9*H*-carbazole (**1**), 9-(6-phenyl-pyridin-3-ylmethyl)-9*H*-carbazole (**3a**), and $Ir(Cz\text{-}ppy)_3$ (**5a**) were synthesized by following the method we reported previously [23].

2.2. Synthesis

9-((6-(4-Fluorophenyl)pyridin-3-yl)methyl)-9*H*-carbazole (3b): Compound **1** (4.68 g, 16 mmol) and tetrakis(triphenylphosphine)palladium(0) ($Pd(PPh_3)_4$, (caution: air sensitive; light sensitive; incompatible with water, strong oxidants) 0.56 g, 0.48 mmol) were dissolved in toluene (50 mL) followed by treating with a degassed solution of K_2CO_3 (4.53 g, 32 mmol) in H_2O (16 mL). Then, the solution of 4-fluorophenylboronic acid (2.79 g, 20 mmol) in EtOH (12 mL) was added dropwise into the mother solution. The mixture was stirred at 85 °C for overnight under Ar gas. After cooling the reaction mixture, it was poured into 100 mL of water and the mixture was extracted with toluene. The combined organic layers were washed with brine and dried over Na_2SO_4. Removal of the solvent under a reduced pressure gave a crude product, which was purified by silica-gel column chromatography (ethyl acetate: chloroform = 1:15) to give a white powder in 90% yield (5.07 g, 14.4 mmol). ^{1}H NMR (400 MHz, $CDCl_3$) δ 8.66 (s, 1H), 8.16 (d, J = 8.0 Hz, 2H), 7.89–7.93 (m, 2H), 7.50 (d, J = 8.0 Hz, 1H), 7.47 (t, J = 8.0 Hz, 2H), 7.40 (d, J = 8.0 Hz, 2H), 7.36 (d, J = 8.0 Hz, 1H), 7.29 (t, J = 8.0 Hz, 2H), 7.12 (t, J = 8.0 Hz, 2H), 5.56 (s, 2H). Anal. Calcd for $C_{24}H_{17}N_2F$: C, 81.80; H, 4.86; N, 7.96. Found: C, 81.92; H, 4.85; N, 7.69.

$Ir(Cz\text{-}ppy)_2(Cz\text{-}Fppy)_1$ (5b): To a solution of **3a** (4.41 g, 13.2 mmol) in 2-ethoxyethanol:H_2O (3:1, 60 mL) was added $IrCl_3 \cdot 3H_2O$ (2.12 g, 6.0 mmol) and the reaction mixture was heated to 120 °C for 24 h. The resulting solution was concentrated at 55 °C and the crude solid was collected. It was washed with 100 mL of water, 50 mL of hexane, and 50 mL of ethyl ether. The crude product was purified by silica-gel column chromatography (CH_2Cl_2) to give a yellow powder (**4a**) in 71% yield (3.87 g, 2.14 mmol).

To a 2-ethoxyethanol (15 mL) solution of **4a** (1.82 g, 1.01 mmol) were added **3b** (0.78 g, 2.21 mmol) and excess K_2CO_3. The reaction mixture was heated to 120 °C for 12 h. After cooling the mixture to room temperature, a dark yellowish precipitate could be filtered off and was washed with 200 mL of methanol and 100 mL of ethyl ether. The crude product was purified by silica-gel column chromatography (hexane: CH_2Cl_2 = 1:4) to give a yellow powder in 48% yield (1.17 g, 0.98 mmol). ^{1}H NMR (400 MHz, $CDCl_3$) δ 8.10–8.14 (m, 6H), 7.29–7.38 (m, 12H), 7.13–7.20 (m, 6H), 7.10 (d, J = 8.0 Hz, 1H), 7.00–7.04 (m, 2H), 6.74–6.81 (m, 6H), 6.60–6.70 (m, 6H), 6.33–6.38 (m, 1H), 6.24–6.28 (m, 3H), 6.15 (s, 1H), 4.71–4.93 (m, 6H). Exact mass (MALDI-TOF) for $[MH]^+$ calcd for $C_{72}H_{50}FIrN_6$: 1210.3710, Found: 1210.2440. Anal. Calcd for $C_{72}H_{50}FIrN_6$: C, 71.44; H, 4.16; N, 6.94. Found: C, 71.48; H, 4.15; N, 6.77.

$Ir(Cz\text{-}ppy)_1(Cz\text{-}Fppy)_2$ (5c): To a solution of **3b** (2.33 g, 6.6 mmol) in 2-ethoxyethanol:H_2O (3:1, 60 mL) was added Iridium (III) Chloride Trihydrate ($IrCl_3 \cdot 3H_2O$; caution: avoid metals, hydroxides, carbonates, cyanides, sulfides, sulfites, formaldehyde; incompatible with strong oxidizing agents). (1.06 g, 3.0 mmol) and the reaction mixture was heated to 120 °C for 24 h. The resulting solution was concentrated at 55 °C and the crude solid was collected. It was washed with 100 mL of water and 100 mL of hexane. The crude product was purified by silica-gel column chromatography (CH_2Cl_2) to give a yellow powder (**4b**) in 65% yield (1.76 g, 0.98 mmol).

To a 2-ethoxyethanol (15 mL) solution of **4b** (1.24 g, 0.67 mmol) was added **3a** (0.49 g, 1.48 mmol) and excess K_2CO_3. The reaction mixture was heated to 120 °C for 12 h. After cooling the mixture to room temperature, a dark yellow precipitate was filtered off and washed with 200 mL of methanol and 100 mL of ethyl ether. The crude product was purified by silica-gel column chromatography (hexane: CH_2Cl_2 = 1:4) to give a yellow powder in 41% yield (0.66 g, 0.56 mmol). ^{1}H NMR (400 MHz, $CDCl_3$) δ 8.08–8.12 (m, 6H), 7.30–7.37 (m, 12H), 7.06–7.15 (m, 4H), 6.92–6.98 (m, 3H), 6.69–6.80 (m, 7H), 6.62 (s, 2H), 6.32–6.37 (m, 2H), 6.19–6.28 (m, 3H), 6.10 (s, 1H), 6.00 (d, J = 8.0 Hz, 2H) 5.88 (s, 1H), 4.74–4.90 (m, 6H). Exact mass (MALDI-TOF) for $[MH]^+$ calcd for $C_{72}H_{49}F_2IrN_6$: 1228.3616, Found: 1228.1944. Anal. Calcd for $C_{72}H_{49}F_2IrN_6$: C, 70.40; H, 4.02; N, 6.84. Found: C, 70.45; H, 4.00; N, 6.68.

$Ir(Cz\text{-}Fppy)_3$ (5d): To a 2-ethoxyethanol (15 mL) solution of **4b** (1.49 g, 0.80 mmol) were added **3b** (0.62 g, 1.78 mmol) and excess K_2CO_3. The reaction mixture was heated to 120 °C for 12 h. After cooling it to room temperature, a dark yellowish precipitate was filtered off and washed with 200 mL of methanol and 100 mL of ether. The crude product was purified by silica-gel column chromatography (hexane: CH_2Cl_2 = 1:4) to give a yellow powder in 56% yield (1.08 g, 0.91 mmol). ^{1}H NMR (400 MHz, $CDCl_3$) δ 8.09–8.14 (m, 6H), 7.32–7.39 (m, 12H), 7.14 (d, J = 8.0 Hz, 3H), 6.92–6.97 (m, 6H), 6.69–6.74 (m, 6H), 6.32–6.39 (m, 3H), 6.20 (d, J = 8.0 Hz, 3H), 5.87 (s, 3H), 4.75–4.88 (m, 6H). Exact mass (MALDI-TOF) for $[MH]^+$ calcd for $C_{72}H_{48}F_3Ir\text{-}N_6$: 1246.3522, Found: 1246.2828. Anal. Calcd for $C_{72}H_{48}F_3Ir\text{-}N_6$: C, 72.52; H, 4.31; N, 7.05. Found: C, 72.39; H, 4.31; N, 6.98.

2.3. Characterization

^{1}H NMR spectra were recorded on a Varian Mercury NMR 400 Hz spectrometer using deuterated chloroform purchased from Cambridge Isotope Laboratories, Inc. Elemental analysis was performed by using an EA1112 (Thermo Electron Corp.) elemental analyzer. Mass analysis was performed on a JMS-AX505WA (JEOL) mass spectrometer. The redox properties of the Ir(III) complexes

were examined by using cyclic voltammetry (Model: EA161 eDAQ). The electrolyte solution employed was 0.10 M tetrabutylammonium hexafluorophosphate (Bu_4NPF_6) in a freshly dried MC. The Ag/AgCl and Pt wire (0.5 mm in diameter) electrodes were utilized as reference and counter electrodes, respectively. The scan rate was at 50 mV/s. Absorption spectra of chloroform solutions were obtained using a UV–vis spectrometer (HP 8453, PDA type) in the wavelength range of 190–1100 nm. PL spectra were recorded with a Hitachi's F-7000 FL Spectrophotometer.

2.4. Crystallography

X-ray data for **5b** and **5c** were collected on a Bruker SMART APEXII diffractometer equipped with graphite monochromated MoKα radiation ($\lambda = 0.71073$ Å). Preliminary orientation matrix and cell parameters were determined from three sets of ω/φ scans at different starting angles. Data frames were obtained at scan intervals of 0.5° with an exposure time of 10 s per frame. The reflection data were corrected for Lorentz and polarization factors. Absorption corrections were carried out using SADABS (Sheldrick, G. M. *SADABS*, *A program for area detector absorption corrections*, University of Göttingen, Germany, 1994.). The structures were solved by direct methods and refined by full-matrix least-squares analysis using anisotropic thermal parameters for non-hydrogen atoms with the SHELXTL (Sheldrick, G. M. *SHELXTL*, version 5, Bruker AXS: Madison, Wisconsin, 1995.) program. All hydrogen atoms were calculated at idealized positions and refined with the riding models.

2.5. Electroluminescence measurement

The multi-layer diodes have a structure of ITO/PEDOT:PSS (40 nm)/PVK:Ir(III) complex or PVK:PBD:Ir(III) complex (40 nm)/BCP (5 nm)/Alq_3(35 nm)/LiF(1 nm)/Al(100 nm). The conducting PEDOT:PSS layer was spin-coated onto the ITO-coated glasses in an argon atmosphere. The emitting layer then was spin-coated onto the thoroughly dried PEDOT layer using the solution (conc: 2.0 wt%) in monochlorobenzene.

For multi-layer devices, 2,9-dimethyl-4,7-diphenyl-1,10-phenanthroline (BCP) and tris(8-hydroxyquinoline) aluminium (Alq_3) layer were vacuum-deposited onto the emitting polymer layer. Finally, LiF (1 nm)/Al (100 nm) electrodes were deposited onto the Alq_3 layer. Current density–voltage characteristics were measured with a Keithley 2400 source meter. The brightness and electroluminescence spectra of the devices were measured with Spectra Colorimeter PR-650.

3. Results and discussion

3.1. Materials synthesis

We demonstrated the synthetic route to the Ir(III) complex Ir(Cz-ppy)$_3$, which contains a carbazolyl substituent, in a previous report [23]. In this study, the 9-((6-(4-fluorophenyl)pyridin-3-yl)methyl)-9*H*-carbazole ligand was newly synthesized for preparing the heteroleptic and homoleptic Ir(III) complexes (see Figs. 1–3). For a new ligand, 9-((6-chloropyridin-3-yl)methyl)-9*H*-carbazole and 4-fluorophenylboronic acid were reacted via the Suzuki coupling method to yield 9-((6-(4-fluorophenyl)pyridin-3-yl)methyl)-9*H*-carbazole (**3b**) in a moderately good yield (>90%) (see Fig. 1).

The structures of Ir(Cz-ppy)$_3$ (**5a**), Ir(Cz-ppy)$_2$(Cz-Fppy)$_1$ (**5b**), Ir(Cz-ppy)$_1$(Cz-Fppy)$_2$ (**5c**), and Ir(Cz-Fppy)$_3$ (**5d**) are illustrated in Figs. 2 and 3. As a reference, in Ir(Cz-ppy)$_3$ [20], the carbazolyl group was attached to the 5-position of the pyridine ring to yield the carbazolyl phenylpyridine ligand (**3a**).

Following the Nonoyama reaction, $IrCl_3 \cdot 3H_2O$ was treated with an excess of ligands (3a or 3b) in a mixed solvent of 2-ethoxyethanol and water (3:1 v/v) to form an iridium dimer (**4a** or **4b**) having chloride bridges. For a ligand exchange reaction, **4a** was treated with a stochiometric amount of 9-((6-(4-fluorophenyl)pyridin-3-yl)methyl)-9*H*-carbazole to yield **5b**. The exchange reaction between the two ligands was successfully performed in this study. The compound **4b** was also reacted with 9-((6-phenylpyridin-3-yl)methyl)-9*H*-carbazole, and the Ir(III) complex, **5c** [Ir(Cz-ppy)$_1$(Cz-Fppy)$_2$], was carefully collected from the mixture by repeated column chromatography. A significant improvement in the solubility of the iridium complex was observed only on introducing the carbazolyl moiety into the conventional ligand in Ir(ppy)$_3$. We examined the solubility difference between conventional Ir(ppy)$_3$ and new Ir(III) complexes. Monochlorobenzene was selected as 4.5 mg, 5.1 mg, 4.0 mg, and 3.8 mg of Ir(Cz-ppy)$_3$, Ir(Cz-ppy)$_2$(Cz-Fppy)$_1$, Ir(Cz-ppy)$_1$(Cz-Fppy)$_2$, and Ir(Cz-Fppy)$_3$ were dissolved in 1 g of monochlorobenzene at room temperature, respectively while only 1 mg of Ir(ppy)$_3$ was barely soluble in hot monochlorobenzene (1 g) under sonication for 1 h. The increased solubility is very beneficial for solution-based device fabrication.

3.2. Structure of Ir(Cz-ppy)$_1$(Cz-Fppy)$_2$ (*5c*) and Ir(Cz-Fppy)$_3$ (*5d*)

A very interesting aspect of the newly synthesized Ir(III) complexes, **5c** and **5d**, involves the determination of their crystal structures. A single crystal was prepared by using a hyperconcentrated monochlorobenzene solution. It was quite intriguing to grow Ir(Cz-ppy)$_1$(Cz-Fppy)$_2$(**5c**) and Ir(Cz-Fppy)$_3$(**5d**) as large single crystals in a solution system. In our previous study, the crystal structure of **5a** was analyzed and it was seen that the three C atoms of the three ligating groups are positioned in a facial configuration. The principal axis of the molecule lies on the pseudo C3 symmetry [24].

The molecular structures of **5c** and **5d** were determined by X-ray crystallography and are illustrated in Fig. 4 [24,25]. Both complexes have distorted octahedral coordination environments and three bulky cyclometalating ligands encircle the Ir centers. As expected, **5c** comprises an unsymmetric core with one Cz-ppy and two F-substituted Cz-ppy, while in **5d**, three Cz-Fppy ligands coordinate to an Ir metal ion. The isomeric arrangements for the central Ir atoms for **5c** and **5d** can be viewed as facial configurations, which is

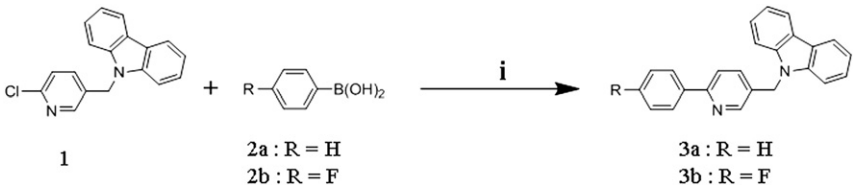

Fig. 1. Synthetic procedure: i) $Pd(PPh_3)_4$, K_2CO_3,Toluene/H_2O/EtOH, 80 °C.

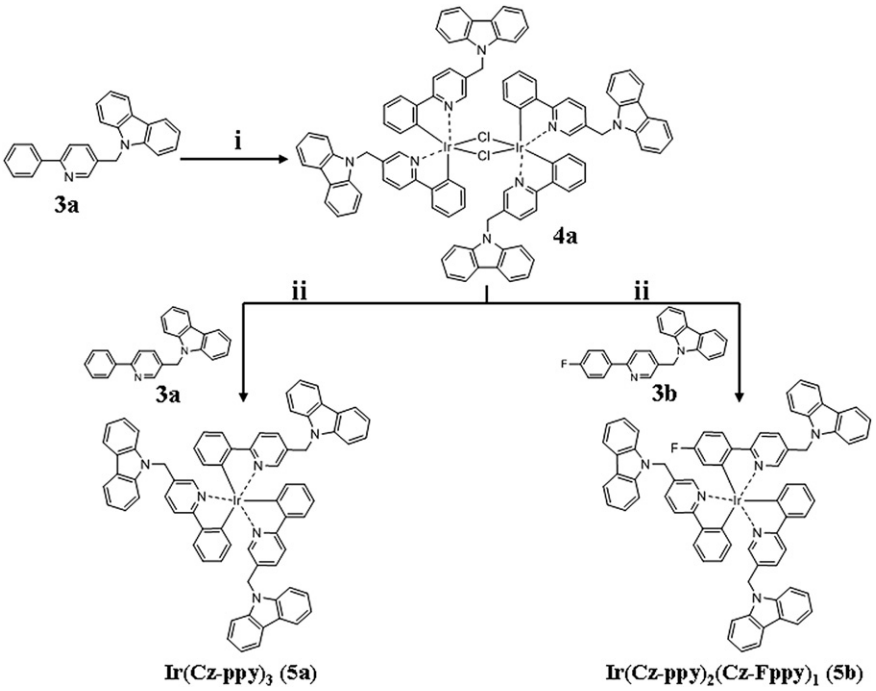

Fig. 2. Synthetic procedure: i) $IrCl_3 \cdot 3H_2O$, 2-ethoxyethanol, H_2O, 120 °C, ii) K_2CO_3, 2-ethoxyethanol, 120 °C.

also found in **5a** constructed from three Cz-ppy ligands without F groups [20]. The Ir-C and Ir-N lengths in **5c** range from 2.007(6) to 2.021(6) Å and from 2.129 to 2.132 Å, respectively, which are similar to those in **5a**. These metrical parameters are more scattered than those of fac-Ir(tpy)$_3$ [tpy = 2-(*p*-tolyl)pyridyl], and bear no long or structurally congested side groups [26]. This may be related to the steric effect stemming from the bulky Cz-ppy ligands. The averaged lengths for **5a** and **5c** were determined as follows; Ir-C = 2.018(9) Å for **5a** and 2.016(8) Å for **5c**; Ir-N = 2.130(8) Å for **5a** and 2.310(1) Å for **5c**. The length of Ir-N for **5c** is a little longer than that for fac-Ir(tpy)$_3$ [Ir-N = 2.132(5) Å] [26]. The observation of the significantly long Ir-N bond length was definitely associated with the trans effect of the phenyl groups. For **5d**, the mean Ir-C and Ir-N bond distances were equal to 2.007(5) and 2.113(6) Å, respectively, which were slightly shorter than those observed in **5a**, **5c**, and tpy-based Ir complexes [26].

The electron-withdrawing F group is placed in a meta position with respect to the C atom bound to Ir. Hence, the electronically inductive effect of F is not strong, which may be responsible for the small reduction in Ir-C and Ir-N for **5d**.

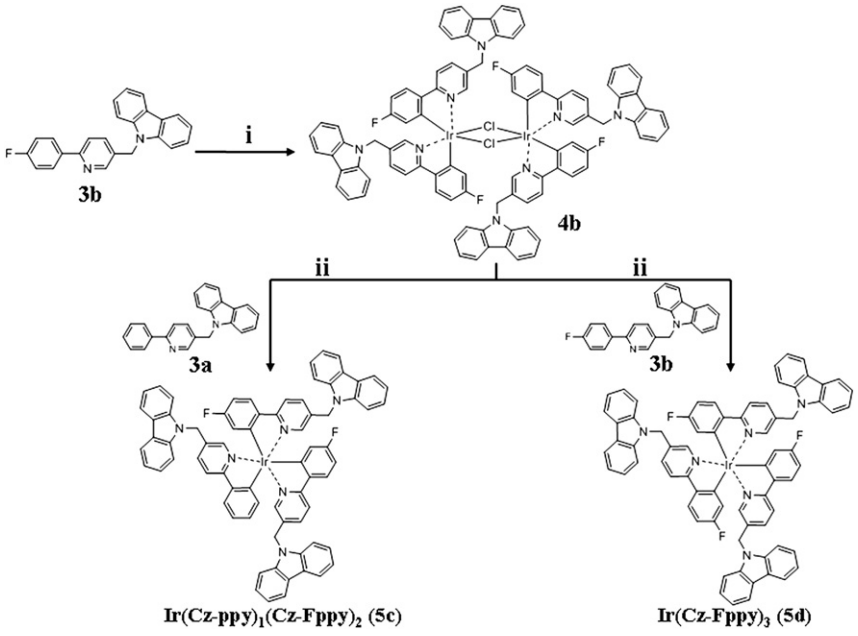

Fig. 3. Synthetic procedure: i) $IrCl_3 \cdot 3H_2O$, 2-ethoxyethanol, H_2O, 120 °C, ii) K_2CO_3, 2-ethoxyethanol, 120 °C.

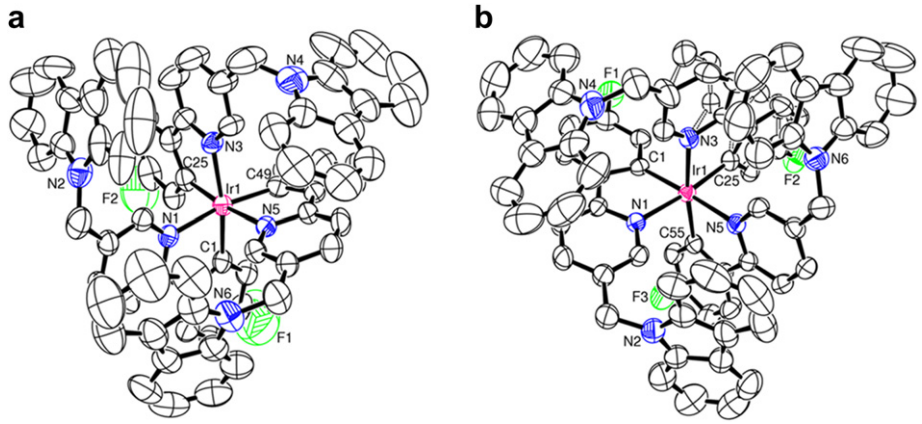

Fig. 4. ORTEP diagrams of 5c and 5d. The thermal ellipsoid for the image represents a 50% probability limit. (a) 5c, (b) 5d.

3.3. UV–vis absorption and the photoluminescent properties of iridium complexes

The absorption and PL spectra of the solution samples of **5a, 5b, 5c**, and **5d** are shown in Fig. 5. The spectral shapes were similar to that observed for $Ir(ppy)_3$, except for a spectral shift. The absorption bands of the spectra of the four carbazolyl substituted phenylpyridine Ir(III) complexes below 320 nm are ascribed to the intra-ligand $\pi-\pi^*$ transitions originating from the Ir-complex, while the absorption at around 342–343 nm is due to the carbazole moieties. In a lower energy region spanning from 380 to 520 nm, we could observe a weak and broad absorption band with shoulders, which can be attributed to spin-allowed and spin-forbidden metal-to-ligand charge transfer (MLCT) transitions of the Ir(III) complexes. The absorption edge was shifted to a lower wavelength with the number of the fluorinated ligand (**3b**), which is due to the variation in the electronic properties of the three ligands. The PL spectra of the Ir(III) complexes in $CHCl_3$ solutions are shown in Fig. 5. They show a spectral shift with ligand modification according to the slight shift in the absorption spectrum. It should be noticed that introducing one 3b instead of **3a** yields a hypsochromic shift of 5 nm in the PL spectrum of $Ir(Cz\text{-}ppy)_2(Cz\text{-}Fppy)_1$, relative to that of the green-emitting $Ir(Cz\text{-}ppy)_3$, ($\lambda_{em} = 520$ nm). It can be considered that the slightly dissimilar excited and ground states were involved in the phosphorescent transition of $Ir(Cz\text{-}ppy)_2(Cz\text{-}Fppy)_1$. When we added one and two more fluorine substituted ligands, the PL spectra of $Ir(Cz\text{-}ppy)_1(Cz\text{-}Fppy)_2$, and $Ir(Cz\text{-}Fppy)_3$ had emission maximums at 510 and 495 nm, respectively. Tethering the fluorine in the phenylpyridine ligand structure had an effect on the optical and photophysical properties.

3.4. Electrochemical analysis

The electrochemical characterizations of these complexes showed that their oxidation was reversible, which is necessary information to determine their electronic energy levels (see Fig. 6). Cyclic voltammograms were recorded on film samples and the potentials were obtained relative to an internal ferrocene reference (Fc/Fc^+). These CV scans in the −2.0 to +2.0 V (vs Ag/AgCl) range showed reversible oxidation peaks. Unfortunately, the reduction behaviors were irreversible; therefore, we were unable to accurately estimate their HOMO and LUMO energies. To determine the LUMO levels, we combined the CV oxidation potential with the optical energy band gap (E_g^{opt}) resulting from the absorption edge in the absorption spectrum. Voltammograms of **5a, 5b, 5c**, and **5d** in their solution states showed that their lowest oxidative waves were at +0.74, +0.75, +0.84, and +0.90 V, respectively. As the density of the fluorine substituted phenylpyridine ligand, **3b**, increased, the oxidative stability improved. As shown in Table 1, **5a**, **5b**, **5c**, and **5d** had HOMO levels of −5.14, −5.15, −5.24, and −5.30 eV, respectively. The HOMO energy levels in **5b**, **5c**, and **5d** became deeper due to the presence of an electron withdrawing substituent in the ligand structure.

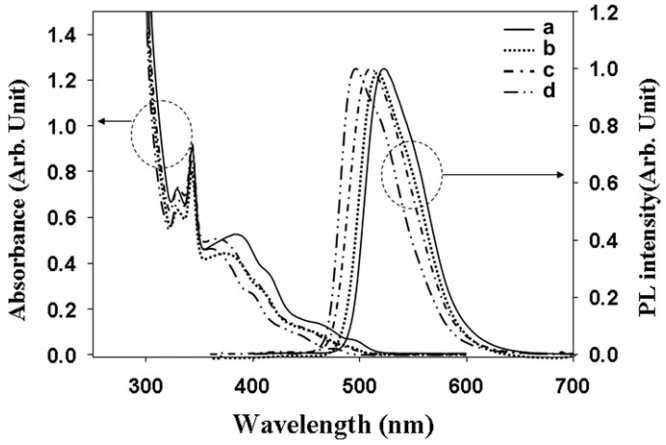

Fig. 5. UV–vis absorption and PL spectra of (a) 5a, (b) 5b, (c) 5c, and (d) 5d in the solution state (solvent: chloroform 4×10^{-6} M).

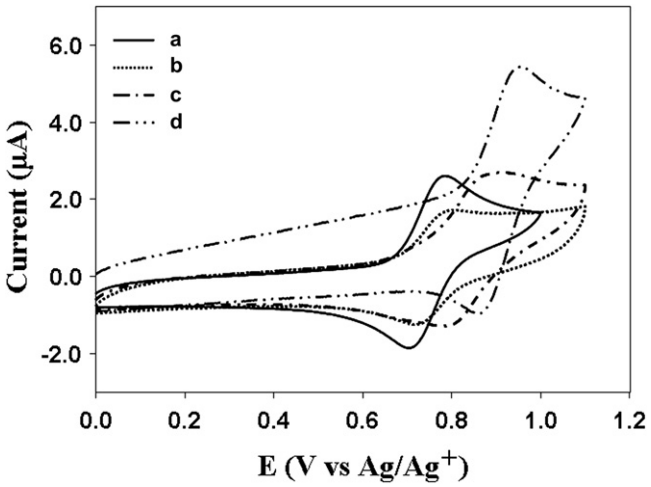

Fig. 6. Cyclic voltammograms of (a) 5a, (b) 5b, (c) 5c, and (d) 5d in the solution state (solvent: methylene chloride).

Table 1
Physical properties of the four different Ir(III) complexes.

Ir(III)-complex	Absorption Wavelength (nm)	λ_{em} (nm)	$E_{ox}^{1/2}$ (V)[a]	HOMO (eV)[b]	LUMO (eV)[c]	E_g (eV)[d]
Ir(Cz-ppy)$_3$	343(Cz), 384, 412, 461, 493	520	0.74	5.14	2.74	2.40
Ir(Cz-ppy)$_2$ (Cz-Fppy)$_1$	342(Cz), 374, 408, 455, 487	515	0.75	5.15	2.70	2.45
Ir(Cz-ppy)$_1$ (Cz-Fppy)$_2$	342(Cz), 367, 401, 441, 478	511	0.84	5.24	2.78	2.46
Ir(Cz-Fppy)$_3$	342(Cz), 361, 395, 438, 473	496	0.90	5.30	2.77	2.53

[a] Oxidation potentials measured by cyclic voltammetry.
[b] HOMO = E_{ox} + 4.4 eV.
[c] LUMO = HOMO − E_g.
[d] E_g estimated from the UV–vis absorption spectra.

3.5. Electrophosphorescent properties

The multi-layer diodes had a structure of ITO/PEDOT:PSS (40 nm)/PVK:PBD with the Ir(III) complex (40 nm)/BCP (5 nm)/Alq_3 (35 nm)/LiF (1 nm)/Al (100 nm), respectively (see Fig. 7). PVK (M_w ~ 90,000, ACROS Co.) was selected as the polymer host, as is usual. We fabricated four different multilayered devices. Devices A, B, C, and D were fabricated using **5a**, **5b**, **5c**, and **5d** (10 wt%) doped into PVK:PBD host. Due to the presence of steric hindrance via the carbazolyl groups, the complexes can be doped at a high concentration (10 wt%) into PVK, for electrophosphorescent devices, without exhibiting significant emission quenching behavior [27].

There was a good overlap between the PL spectrum of PVK:PBD (30 wt%) and the metal–ligand charge transfer MLCT absorption bands of the iridium complexes [8,22]. This overlap should enable efficient energy transfer from the singlet-excited state in the host to the MLCT band of the guest.

To emphasize the effect of the PBD on the electrophosphorescence, we also added the performance data of the devices (e.g. devices 1, 2, 3, and 4) without PBD to Table 2.

The current density–voltage luminance curves of the four devices are shown in Fig. 8. The turn-on voltages for these devices were typical for Ir(III) complex doped PLEDs, falling in the 4.5–5.0 V range.

The devices were fabricated under identical conditions during the same period and at least five devices were characterized to provide reproducible performance data, which are tabulated in Table 2. The maximum brightness values of the LEDs were around 20,250 cd/m^2 (at 2018.7 A/m^2) for device A, 25,520 cd/m^2 (at 2978.2 A/m^2) for device B, 17520 cd/m^2 (at 1816.3 A/m^2) for device C, and 9501 cd/m^2 (at 2154.5 A/m^2) for device D. These brightness levels could not be compared and explained in an appropriate way since the emission color coordinates were somewhat different from each other. However, an enhancement of the brightness was clearly observed when PBD was added to the PVK. Compared to device A, the other three devices (B, C, D) showed higher current flows under an identical bias voltage, which might be attributed to a lessening of the charge trapping effect arising from the deeper HOMO levels.

Fig. 9 displays the dependence of the luminous efficiency and external quantum efficiency on the current density for the four electrophosphorescent devices. The maximum luminous efficiencies of devices A, B, C, and D were determined to be 19.24 cd/A (at 14.0 A/m^2, η_{EQE} = 8.68%), 16.69 cd/A (at 34.1 A/m^2, η_{EQE} = 5.72%), 20.25 cd/A (at 101.1 A/m^2, η_{EQE} = 6.80%), and 13.87 cd/A (at 35.1 A/m^2, η_{EQE} = 5.77%), respectively. It should be pointed out that the triplet state of the PVK (T_1 = 2.50 eV) was higher in energy than that of the Ir(III) complexes (T_1 = 2.40–2.46 eV), except for Ir(Cz-Fppy)$_3$ (T_1 = 2.53 eV). There were subtle differences between the efficiencies of the three samples, which cannot be explained using the molecular energy levels. However, according to the literature [14], the addition of an electron withdrawing substituent into the ligand raises the LUMO energy level of the Ir(III) complex and less efficient electron trapping in the PVK host might occur due to this shallow LUMO energy level. The triplet energy of Ir(Cz-Fppy)$_3$ was 2.53 eV, which was close to that of PVK, which may have undergone an endothermic triplet–triplet energy transfer from the PVK host to the Ir(III) complex [14].

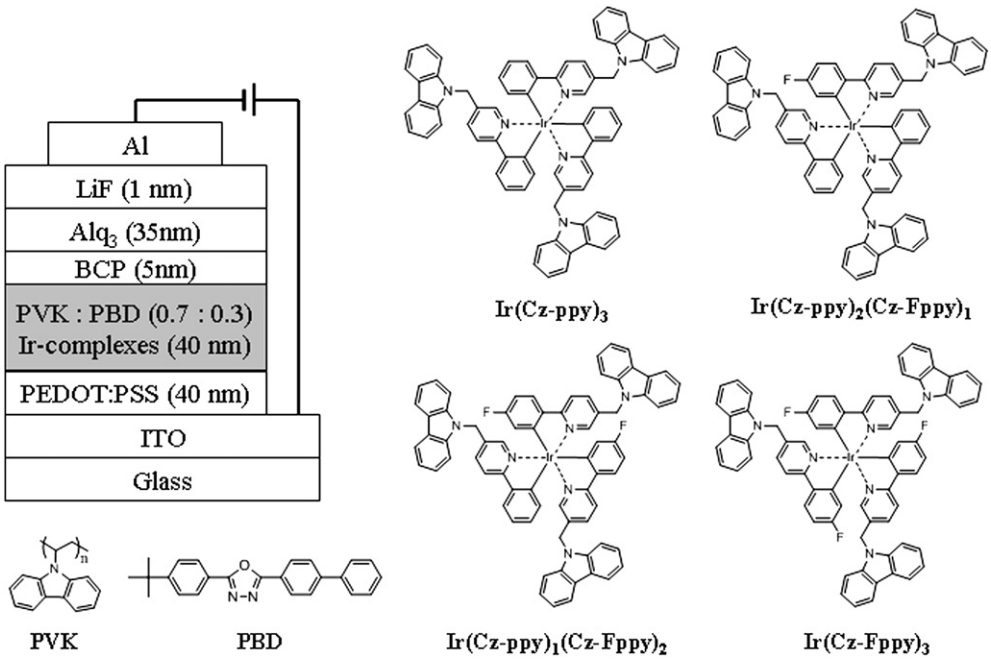

Fig. 7. Molecular structures of Ir(III) complexes, PVK, and PBD. The device configuration of the electrophosphorescent PLED.

Table 2
Measured parameters of the electrophosphorescent devices.

Device	Turn-on (V)	L_{mm}/cd m^{-2} (J)[a]	LE_{max}/cd A^{-1} (J)[a]	PE_{max}/lm W^{-1} (J)[a]	EQE_{max}/%(J)[a]	EL λ_{max}[b] (nm)	CIE coordinate[b] (x, y)
Device I[c]	4	12,820 (1665.4)	15.53 (2.39)	4.64 (2.39)	4.90 (2.39)	528	0.37, 0.58
Device 2[c]	4	10,060 (1670.4)	11.33 (9.41)	3.95 (9.41)	3.89 (9.41)	518	0.32, 0.59
Device 3[c]	4.5	7605 (1665.1)	7.96 (12.86)	3.05 (7.67)	2.72 (7.67)	516	0.30, 0.59
Device 4[c]	4.5	5983 (1764.2)	4.55 (37.06)	1.80 (12.61)	1.83 (12.61)	494	0.25, 0.53
Device A	5	20,250 (2018.7)	19.24 (1.40)	7.55 (1.40)	8.68 (1.40)	520	0.35, 0.60
Device B	4.5	25,520 (2978.2)	16.69 (3.41)	6.99 (3.41)	5.72 (3.41)	512	0.31, 0.60
Device C	4.5	17,520 (1816.3)	20.25 (10.11)	7.22 (3.37)	6.80 (10.11)	512	0.30, 0.60
Device D	4.5	9501 (2154.5)	13.87 (3.51)	6.22 (3.51)	5.77 (3.51)	492	0.25, 0.54

[a] Corresponding J(A/m^2).
[b] At maximum luminance.
[c] ITO/PEDOT:PSS(40 nm)/PVK:Ir(III) complex(40 nm)/BCP(5 nm)/Alq_3(35 nm)//LiF/Al.

It is well known that PVK can be blended with PBD to improve the balance of the electron and hole transporting properties [28–30]. A well-balanced charge-carrier injection and the transport and confinement of the emissive triplet excitons within the emission layer could be achieved, resulting in a significant improvement in the stability of the device efficiency. Due to the presence of a carbazolyl peripheral moiety around the iridium core, the present device had a much slower decrease in efficiency with an increase in current density, thereby suppressing triplet–triplet annihilation. The relatively poor stability of the efficiency in device D was also attributed to a possible backward energy transfer from the PVK host to Ir(Cz-Fppy)$_3$, which is not usual in other devices [14].

Fig. 10 shows the EL emission spectra of the four devices. The spectra of the four devices were quite similar to the PL solution spectra of each Ir(III) complex (see Fig. 5). This suggests that the same excited state specie was responsible for both the PL and EL emissions, resulting from the triplet emission due to the Ir(III) complex. The EL emission was dominated by an Ir(III) complex emission peak at around 520–492 nm. No host emission was observed in the fabricated devices. This seems to indicate that energy transfer from the PVK:PBD host to the four Ir(III) complexes was quite efficient at the optimized dopant concentration of the experiment.

The effect of the 9-((6-(4-fluorophenyl)pyridin-3-yl)methyl)-9*H*-carbazole ligand on the spectral shift to a shorter wavelength induced a variation in the green emission color. The synthetic strategy to add the fluorine substituted phenylpyridine ligand to

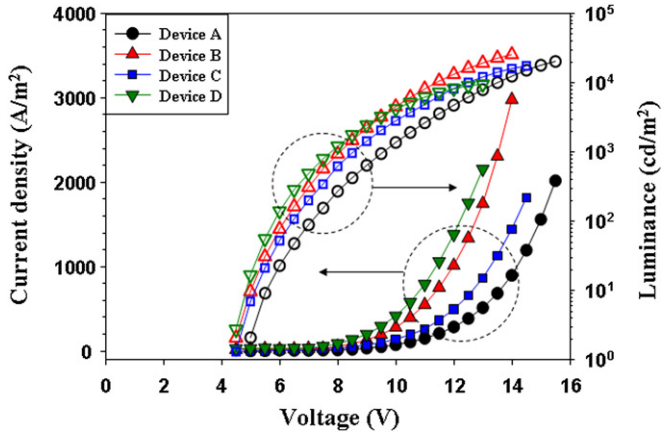

Fig. 8. Dependence of current density and luminance on the applied voltage. Open symbol: Luminance; Filled symbol: Current density.

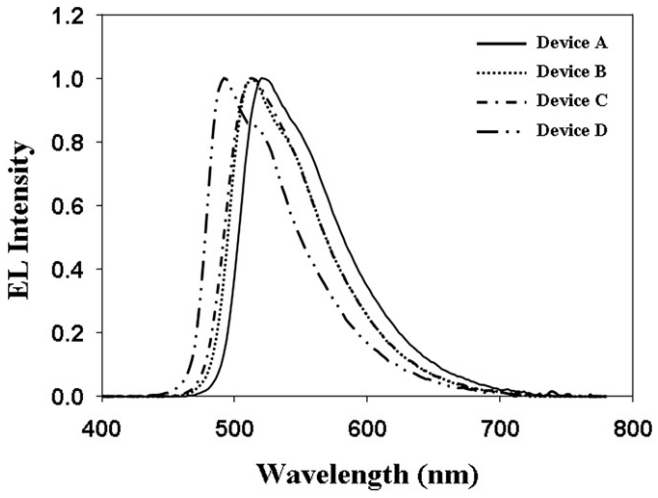

Fig. 10. EL spectra of the four electrophosphorescent devices.

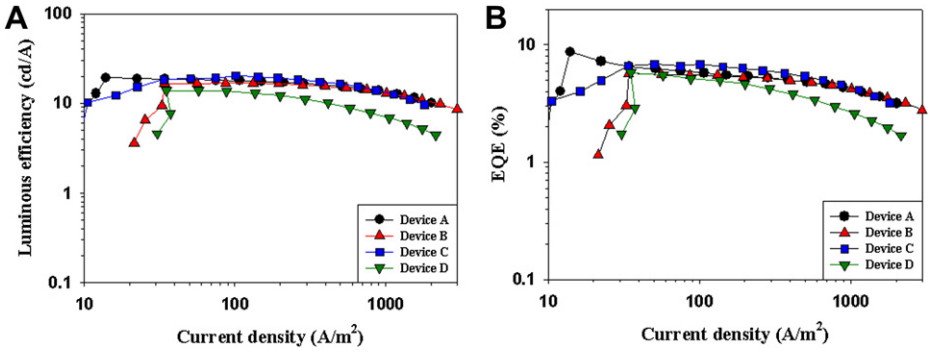

Fig. 9. Dependence of luminous efficiency and external quantum efficiency on the current density.

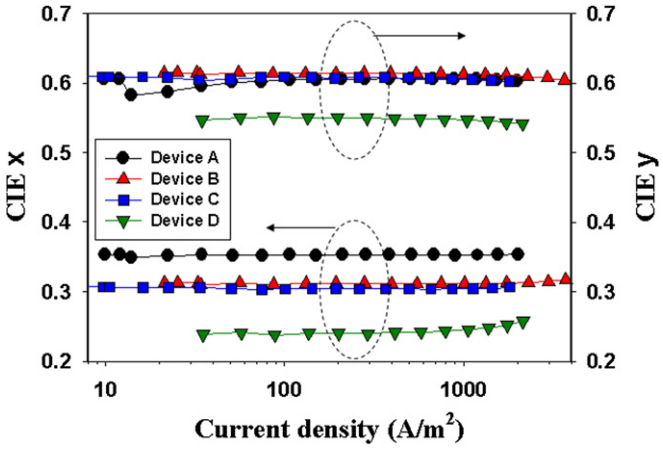

Fig. 11. Stability of the chromaticity depicted by CIE coordination.

the Ir(III) complex successfully tuned the color coordinate precisely, which was evidenced by the CIE coordinates (see Fig. 10 and Table 2). Thus, it can be explained in greater detail by using the differences in the electronic properties of the 9-((6-phenylpyridin-3-yl)methyl)-9*H*-carbazole and 9-((6-(4-fluorophenyl)pyridin-3-yl)methyl)-9*H*-carbazole ligands.

Fig. 11 shows the current density dependence of the chromaticity, which was used to evaluate its stability. When the EL spectrum was converted into chromaticity coordinates on the CIE 1931 diagram, we could observe the evident stability of the chromaticity with an increase in the applied voltage, concomitantly with an increase in the current density. Therefore, the stability of the color coordinate was also improved by introducing the electron transport molecule.

4. Conclusions

The new soluble iridium complexes, Ir(Cz-ppy)$_2$(Cz-Fppy)$_1$, Ir(Cz-ppy)$_1$(Cz-Fppy)$_2$, and Ir(Cz-Fppy)$_3$ were successfully synthesized, and their electrophosphorescence device performances were evaluated using a PVK:PBD blend host. The Ir(III) complexes had good solubility over Ir(ppy)$_3$, thus possessing greater processability.

It was intriguing that introducing one **3b** instead of **3a** yielded a hypsochromic shift of 5 nm in the PL spectrum of Ir(Cz-ppy)$_2$(Cz-Fppy)$_1$, relative to that of the green-emitting Ir(Cz-ppy)$_3$, (λ_{em} = 520 nm). When we added one and two more fluorine substituted ligands, the PL spectra of Ir(Cz-ppy)$_1$(Cz-Fppy)$_2$ and Ir(Cz-Fppy)$_3$ had emission maximums at 510 and 495 nm, respectively.

The efficiencies of all of the devices were shown to be quite promising compared to other similar, conventional devices made of Ir(ppy)$_3$. In particular, with the variation of the ligand composition, the PL emission and electrophosphorescence displayed quite unique characteristics. The color coordinate of the device was finely tuned by adding the fluorine substituted phenylpyridine ligand into the Ir(III) complex. Our work unambiguously demonstrated that new highly soluble Ir(III) complexes that take advantage of efficient excited energy transfer can be fully utilized for tuning the emission properties of phosphorescent EL devices.

Acknowledgments

This research work was supported by LG display (2009–2010). Particularly, Prof. D. H. Choi thanks the financial support by the Seoul R&BD Program (2008–2009), and second stage of the Brain Korea 21 Project in 2009 (Korea Research Foundation)

References

[1] Yersin H. Highly efficient OLEDs with phosphorescent materials. Weinheim Germany: Wiley-VCH; 2007.
[2] Adachi C, Baldo MA, Thompson ME, Forrest SR. Nearly 100% internal phosphorescence efficiency in an organic light-emitting device. Journal of Applied Physics 2001;90:5048–51.
[3] Baldo MA, O'Brien DF, You Y, Shoustikov A, Sibley S, Thompson ME, et al. Highly efficient phosphorescent emission from organic electroluminescent devices. Nature 1998;395:151–4.
[4] Tsutsui T, Yang M-J, Yahiro M, Nakamura K, Watanabe T, Tsuji T, et al. High quantum efficiency in organic light-emitting devices with iridium-complex as a triplet emissive center. Japanese Journal of Applied Physics 1999;38:L1502–4.
[5] Ostrowski JC, Robinson MR, Heeger AJ, Bazan GC. Amorphous iridium complexes for electrophosphorescent light emitting devices. Chemical Communications 2002:784–5.
[6] Duan JP, Sun PP, Cheng CH. New iridium complexes as highly efficient orange-red emitters in organic light-emitting diodes. Advanced Materials 2003;15:224–8.
[7] Beeby A, Bettington S, Samuel IDW, Wang Z. Tuning the emission of cyclometalated iridium complexes by simple ligand modification. Journal of Materials Chemistry 2003;13:80–3.
[8] Gong X, Robinson MR, Ostrowski JC, Moses D, Bazan GC, Heeger AJ. High-efficiency polymer-based electrophosphorescent devices. Advanced Materials 2002;14:581–5.
[9] Ikai M, Tokito S, Sakamoto Y, Suzuki T, Taga Y. Highly efficient phosphorescence from organic light-emitting devices with an exciton-block layer. Applied Physics Letters 2001;79:156–8.
[10] Xia Z-Y, Xiao X, Su J-H, Chang C-S, Chen CH, Li D-L, et al. Low driving voltage and efficient orange-red phosphorescent organic light-emitting devices based on a benzotriazole iridium complex. Synthetic Metals 2009;159:1782–5.
[11] Xu Z, Li Y, Ma X, Gao X, Tian H. Synthesis and properties of iridium complex based 1,3,4-oxadiazoles derivatives. Tetrahedron 2008;64:1860–7.
[12] Huang W-S, Lin JT, Lin H-C. Green Phosphorescent iridium dendrimers containing dendronized benzoimidazole-based ligands for OLEDs. Organic Electronics 2008;9:557–68.
[13] Bettington S, Tavasli M, Bryce MR, Beeby A, Al-Attar H, Monkman AP. Tris-cyclometalated iridium(III) complexes of carbazole(fluorenyl)pyridine ligands: synthesis, redox and photophysical properties, and electrophosphorescent light-emitting diodes. Chemistry-A European Journal 2007;13:1423–31.
[14] Liu H–M, Wang P–F, He J, Zheng C, Zhang X–H, Chew S–L, et al. High-efficiency endothermic energy transfer in polymeric light-emitting devices based on cyclometalated Ir complexes. Applied Physics Letters 2008;92:023301.
[15] Anthopoulos TD, Frampton MJ, Namdas EB, Burn PL, Samuel IDW. Solution-processable red phosphorescent dendrimers for light-emitting device applications. Advanced Materials 2004;16:557–60.
[16] King SM, Al–Attar HA, Evans RJ, Congreve A, Beeby A, Monkman AP. The use of substituted iridium complexes in doped polymer electrophosphorescent devices: the influence of triplet transfer and other factors on enhancing device performance. Advanced Functional Materials 2006;16:1043–50.
[17] Lo SC, Richards GJ, Markham JPJ, Namdas EB, Sharma S, Burn PL, et al. A light-blue phosphorescent dendrimer for efficient solution-processed light–emitting diodes. Advanced Functional Materials 2005;15:1451–8.
[18] Xie HZ, Liu MW, Wang OY, Zhang XH, Lee CS, Hung LS, et al. Reduction of self-quenching effect in organic electrophosphorescence emitting devices via the use of sterically hindered spacers in phosphorescence molecules. Advanced Materials 2001;13:1245–8.
[19] Wong WY, Ho CL, Gao ZQ, Mi BX, Chen CH, Cheah KW, et al. Multifunctional iridium complexes based on carbazole modules as highly efficient electrophosphors. Angewandte Chemie International Edition 2006;45:7800–3.
[20] Wong WY, Zhou GJ, Yu XM, Kwok HS, Tang BZ. Amorphous diphenylamino-fluorene-functionalized iridium complexes for high-efficiency electrophosphorescent light-emitting diodes. Advanced Functional Materials 2006;16:838–46.
[21] You Y, An C–G, Lee D–S, Kim J-J, Park SY. Silicon-containing dendritic tris-cyclometalated Ir(III) complex and its electrophosphorescence in a polymer host. Journal of Materials Chemistry 2006;16:4706–13.
[22] Liu H–M, He J, Wang P–F, Xie H–Z, Zhang X–H, Lee C–S, et al. High-efficiency polymer electrophosphorescent diodes based on an Ir (III) complex. Applied Physics Letters 2005;87:221103.
[23] Cho MJ, Kim JI, Hong CS, Kim YM, Park YW, Ju B–K, et al. Highly soluble green-emitting Ir(III) complexes with 9-(6-phenyl-pyridin-3-ylmethyl)-9 *H*-carbazole ligands and their application to polymer light-emitting diodes. Journal of Polymer Science Polymer Chemistry Edition 2008;46:7419–28.
[24] Crystal data for Ir(Cz-ppy)$_1$Ir(Cz-Fppy)$_2$: $C_{72}H_{49}F_2IrN_6$, Fw.=.1228.36, monoclinic, space group $P2_1/c$, a = 15.7313(14) b = 13.9434(12) c = 25.414(2) Å, β = 99.563(3)°, V = 5497.10(8) Å^3, Z = 4, D_{calc} = 1.484.g.cm^{-3}, 82143 reflections collected, 13547 unique (Rint = 0.1232), R1 = 0.0493, wR2.=.0.0938, Final R indices [I>2sigma(I)]. CCDC 709485.
[25] Crystal data for Ir(Cz-Fppy)$_3$: $C_{72}H_{48}F_3Ir$-N_6, Fw = 1246.35, monoclinic, space group $P2_1/n$, a = 15.8583(4) *b* = 15.8707(5) *c* = 25.5745(9) Å, = β106.434(2)°, V = 6173.7(3) Å^3, *Z* = 4, D_{calc} = 1.462 g cm^{-3}, 61540 reflections collected, 15306 unique (R_{int} = 0.0344), *R*1 = 0.0279, wR2 = 0.0588, Final R indices [I > 2sigma(I)]. CCDC 709486.

[26] Tamayo AB, Alleyne BD, Djurovich PI, Lamansky S, Tsyba I, Ho NN, et al. Synthesis and characterization of facial and meridional tris-cyclometalated iridium(III) complexes. Journal of the American Chemical Society 2003;125:7377–87.
[27] Chew SL, Lee CS, Lee ST, Wang PF, He J, Li W, et al. Photoluminescence and electroluminescence of a new blue-emitting homoleptic iridium complex. Applied Physics Letters 2006;88:093510.
[28] Pai DM, Yanus JF, Stolka M. Trap-controlled hopping transport. Journal of Physical Chemistry 1984;88:4714–7.
[29] Yang XH, Neher D. Polymer electrophosphorescence devices with high power conversion efficiencies. Applied Physics Letters 2004;84:2476–8.
[30] Yang XH, Neher D, Hertel D, Däubler TK. Highly efficient single-layer polymer electrophosphorescent devices. Advanced Materials 2004;16: 161–6.